Overexpression of the Adiponectin Receptor AdipoR1 in Rat Skeletal Muscle Amplifies Local Insulin Sensitivity

S. A. Patel, K. L. Hoehn, R. T. Lawrence, L. Sawbridge, N. A. Talbot, J. L. Tomsig, N. Turner, G. J. Cooney, J. P. Whitehead, E. W. Kraegen, and M. E. Cleasby

Department of Comparative Biomedical Sciences (S.A.P., L.S., N.A.T., M.E.C.), Royal Veterinary College, University of London, London NW1 0TU, United Kingdom; Department of Pharmacology (K.L.H., R.T.L., J.L.T.), University of Virginia Health System, Charlottesville, Virginia 22908; Diabetes and Obesity Research Program (N.T., G.J.C., E.W.K., M.E.C.), Garvan Institute of Medical Research, and St. Vincent's Hospital Clinical School (N.T., G.J.C.) and School of Medical Sciences (E.W.K.), Faculty of Medicine, University of New South Wales, Sydney, New South Wales 2010, Australia; and Department of Metabolic Medicine (J.P.W.), Mater Medical Research Institute, South Brisbane, Queensland 4101, Australia

Adiponectin is an adipokine whose plasma levels are inversely related to degrees of insulin resistance (IR) or obesity. It enhances glucose disposal and mitochondrial substrate oxidation in skeletal muscle and its actions are mediated through binding to receptors, especially adiponectin receptor 1 (AdipoR1). However, the *in vivo* significance of adiponectin sensitivity and the molecular mechanisms of muscle insulin sensitization by adiponectin have not been fully established. We used *in vivo* electrotransfer to overexpress AdipoR1 in single muscles of rats, some of which were fed for 6 wk with chow or high-fat diet (HFD) and then subjected to hyperinsulinemic-euglycemic clamp. After 1 wk, the effects on glucose disposal, signaling, and sphingolipid metabolism were investigated in test *vs.* contralateral control muscles. AdipoR1 overexpression (OE) increased glucose uptake and glycogen accumulation in the basal and insulin-treated rat muscle and also in the HFD-fed rats, locally ameliorating muscle IR. These effects were associated with increased phosphorylation of insulin receptor substrate-1, Akt, and glycogen synthase kinase-3β. AdipoR1 OE also caused increased phosphorylation of p70S6 kinase, AMP-activated protein kinase, and acetyl-coA carboxylase as well as increased protein levels of adaptor protein containing pleckstrin homology domain, phosphotyrosine binding domain, and leucine zipper motif-1 and adiponectin, peroxisome proliferator activated receptor-γcoactivator-1α, and uncoupling protein-3, indicative of increased mitochondrial biogenesis. Although neither HFD feeding nor AdipoR1 OE caused generalized changes in sphingolipids, AdipoR1 OE did reduce levels of sphingosine 1-phosphate, ceramide 18:1, ceramide 20:2, and dihydroceramide 20:0, plus mRNA levels of the ceramide synthetic enzymes serine palmitoyl transferase and sphingolipid Δ-4 desaturase, changes that are associated with increased insulin sensitivity. These data demonstrate that enhancement of local adiponectin sensitivity is sufficient to improve skeletal muscle IR. **(*Endocrinology* 153: 5231–5246, 2012)**

Glucose uptake by skeletal muscle accounts for 75–80% of normal insulin-stimulated whole-body glucose disposal after a meal. This process is substantially impaired as a result of local insulin resistance (IR) in type 2 diabetes (T2D) and the metabolic syndrome. The typical association of this syndrome with obesity suggests that an altered signal associated with or generated from expanded adipose tissue is involved in muscle IR. This might involve elevated plasma fatty acids (FAs), which cause IR by being ectopically deposited in muscle as triacylglycerol, diacylglyerol, or ceramides (1–3), or altered secretion or action of substances produced by adipose, which influence muscle metabolism (adipokines) (4, 5).

ISSN Print 0013-7227 ISSN Online 1945-7170
Printed in U.S.A.
Copyright © 2012 by The Endocrine Society
doi: 10.1210/en.2012-1368 Received April 3, 2012. Accepted August 20, 2012.
First Published Online September 4, 2012

Abbreviations: ACC, Acetyl-coA carboxylase; AdipoR1, adiponectin receptor 1; AMPK, AMP-activated protein kinase; APPL1, adaptor protein containing pleckstrin homology domain, phosphotyrosine binding domain, and leucine zipper motif-1; CAMKKβ, calmodulin-dependent protein kinase kinase-β; CS, ceramide synthase; FA, fatty acid; GIR, glucose infusion rate; GSK, glycogen synthase kinase; HEC, hyperinsulinemic-euglycemic clamp; HFD, high-fat diet; HSP, high-speed pellet; IR, insulin resistance; IRS1, insulin receptor substrate-1; IVE, *in vivo* electrotransfer; LC-MS, liquid chromatography-mass spectrometry; OE, overexpression; PGC, peroxisome proliferator activated receptor-γ coactivator; PI3-kinase, phosphatidylinositol 3-kinase; R_d, glucose disposal; S1P, sphingosine-1 phosphate; SPTS, serine palmitoyl transferase; TCM, tibialis cranialis muscle; T2D, type 2 diabetes; UCP, uncoupling protein.

Adiponectin is a multimeric adipokine whose secretion is reciprocally related to both adiposity and insulin resistance in humans (6, 7). A role for adiponectin in skeletal muscle has been suggested by its direct effects on glucose disposal in cultured myotubes (8) and lipid oxidation in skeletal muscle strips *ex vivo* (9). However, given the very high plasma concentration of adiponectin (ug/ml) (10) *vs.*, for example, leptin (ng/ml) (11), adiponectin action seems more likely to be primarily determined by receptor abundance or postreceptor signaling events than by ligand concentration alone. Support for this contention comes from studies demonstrating adiponectin resistance in muscles from high-fat diet (HFD)-fed rats (9) and insulin receptor knockout mice (12). The cellular effects of adiponectin are believed to be principally mediated through binding to plasma membrane-associated adiponectin receptors (AdipoRs)-1 and -2 of the progestin and AdipoQ receptor family, of which AdipoR1 is the more abundant isoform in muscle (13, 14). Disruption of AdipoR1 in mice resulted in obesity and impaired glucose tolerance (15) or insulin resistance, associated with increased tissue triglycerides, inflammation, and oxidative stress (16), whereas a muscle-specific knockout was characterized by insulin resistance related to mitochondrial defects (17). The postreceptor signaling events involved in its metabolic effects are less well characterized, although recent work from us (18) and others (19) has suggested a role for adaptor protein containing pleckstrin homology domain, phosphotyrosine binding domain, and leucine zipper motif-1 (APPL1) in mediating an insulin-sensitizing effect of adiponectin.

Considerable evidence has implicated AMP-activated protein kinase (AMPK) as a principal effector of adiponectin in muscle (20–22) and activation of calmodulin-dependent protein kinase kinase-β (CAMKKβ) in response to an AdipoR1-associated extracellular calcium influx has recently been suggested as the means whereby AMPK is activated (17). However, recent work from the Scherer laboratory questioned the primacy of AMPK in the mechanism of adiponectin action, based on the use of the relatively unphysiological globular form of adiponectin in many studies, plus the finding that AMPK was dispensable for the glucose-lowering effects of adiponectin (14). Data were provided showing that a ceramidase activity inherent to the AdipoRs was fundamental to adiponectin's effects, through a reduction in ceramide and an increase in antiapoptotic sphingosine-1 phosphate (S1P) levels, and hypothesized that a resulting release of calcium from the endoplasmic reticulum might activate AMPK downstream via CAMKKβ. Nevertheless, it is still unclear whether an altered sphingolipid profile is a key mechanistic component of the insulin-sensitizing effects of adiponectin *in vivo* and indeed whether enhancing adiponectin sensitivity at the tissue level might provide a viable additional approach to therapy of T2D and the metabolic syndrome.

Here we aimed to determine in rats *in vivo*, using an acute method of muscle-specific AdipoR1 overexpression (OE), whether increasing adiponectin sensitivity in muscle would improve glucose disposal and insulin sensitivity and whether this effect would be sufficient to overcome the lipid-associated IR induced by a HFD. We then aimed to establish the molecular mechanisms for the observed effects, with particular emphasis on establishing the effects of AdipoR1 on muscle sphingolipid profile.

Materials and Methods

Materials

General reagents were supplied by Sigma-Aldrich (Gillingham, UK) and molecular reagents by Promega (Southampton, UK). The AdipoR1 cDNA was purchased from Origene (Cambridge BioScience, Cambridge, UK) and pCAGGs vector was a kind gift from Professor D. Wells (Royal Veterinary College) (23). APPL1 antibody was kindly supplied by Professor A. Xu (University of Hong Kong) (24) and AdipoR antibodies by Astra Zeneca (Mölndal, Sweden) (15). pY608-insulin receptor substrate-1 (IRS1) antibody was from Biosource International (Camarillo, CA); uncoupling protein (UCP)-3 antibody from Thermo Scientific (Rockford, IL); antiperoxisome proliferator activated receptor-γ coactivator (PGC)-1α from Calbiochem (Merck Chemicals, Nottingham, UK); total glycogen synthase kinase (GSK)-3α/β, total IRS1, and pT642- and total TBC1D4 antibodies from Millipore (Billerica, MA); β-actin and adiponectin antibodies from Sigma; caveolin-1 antibody from Santa Cruz Biotechnology (Santa Cruz, CA); and all others from Cell Signaling Technology (Beverley, MA).

Vector construction

pCMV6-AdipoR1 was consecutively digested with *Sma*I and *Bam*HI, and the cDNA insert agarose gel was separated and extracted using a QIAquick gel extraction kit (QIAGEN, Crawley, UK). Overhanging ends were subsequently filled in using T4 DNA polymerase, and *Eco*RI adaptors were ligated to the blunt-ended product. Excess adaptors were removed by passage through a column containing Sephacryl-S400 resin and the cDNA was ligated into dephosphorylated *Eco*RI-linearized pCAGG vector. The product was used to transform competent JM109

Escherichia coli and correct insertion of cDNA into clones was verified by *Bgl*II digestion and sequencing of minipreps derived from colonies.

Animals

All experimental procedures were approved by the Royal Veterinary College's Ethics and Welfare Committee and were carried out under a U.K. Home Office license to comply with the Animals (Scientific Procedures) Act 1986.

Male Wistar rats were obtained from Charles River (Margate, UK). Animals were maintained at 22 ± 0.5 C under a 12-h day, 12-h night cycle and fed standard maintenance chow (rat and mouse diet 1; Lillico, Betchworth, UK) *ad libitum*. Where a HFD was used, half of the rats were fed RD12492, contributing 60% of calories from fat (lard), 20% from protein, and 20% from carbohydrate (Research Diets Inc., New Brunswick, NJ) for 6 wk *ad libitum*, a period sufficient to generate muscle insulin resistance without pronounced obesity (25). One week before basal glucose uptake or hyperinsulinemic-euglycemic clamp (HEC) study, one or both jugular veins were cannulated, as previously described (18). Isofluorane anesthesia was supplemented with local bupivacaine irrigation (0.5 mg per 100 g) and 5 mg/kg sc carprofen to provide analgesia. Only those rats that had recovered their presurgery weight were studied. Rats were euthanased using pentobarbitone, followed by rapid dissection and freeze-clamping of muscles.

In vivo electrotransfer (IVE)

IVE was performed under anesthesia and simultaneous with cannulation surgery where applicable. Preparation and injection of DNA and electrotransfer was carried out as described (26), with 2 × 0.25 ml injections of 120 IU/ml hyaluronidase (Sigma) administered to each muscle 2 h before IVE. Tibialis cranialis muscles (TCMs) were injected percutaneously with six spaced 50-μl aliquots of DNA prepared in endotoxin-free sterile saline (QIAGEN Mega-Prep kit) at 0.5 mg/ml. Right TCMs were injected with pCAGGs-AdipoR1 and left TCMs with empty pCAGGs vector as a within-animal control. Immediately afterward, one 800-V/cm, 100-μsec electrical pulse and four 80-V/cm, 100-msec pulses at 1 Hz were administered across the distal limb via tweezer electrodes attached to an ECM-830 electroporator (BTX, Holliston, MA).

Assessment of *in vivo* glucose metabolism in rats under basal and hyperinsulinemic-euglycemic clamp conditions

Conscious rats were studied after 5–7 h fasting. Jugular cannulae were connected to infusion and/or sampling lines and the rats left to acclimatize for 30–40 min. HECs were conducted as described (27), using a constant insulin infusion of 2.5 U/h, commensurate with the generation of normal postprandial plasma levels. Blood was withdrawn approximately every 10 min for the determination of glucose using a YSI 2300 glucose/lactate analyzer (YSI Life Sciences, Yellow Springs, OH) and the infusion rate of 50% glucose adjusted to maintain euglycemia. A combined bolus injection of 2-[1,2-^{3}H (N)]deoxy-D-glucose and D-[U-^{14}C]glucose (NEN Life Science Products/PerkinElmer, Waltham, MA) was administered immediately or once steady-state euglycemia was achieved in clamped animals, 45 min before the end. Plasma glucose tracer disappearance was used to calculate basal or clamp whole-body glucose disposal (R_d). In clamped animals, endogenous glucose output was derived from the difference between R_d and the net glucose infusion rate (GIR). The area under the tracer disappearance curve of 2-deoxy-D-[2,6,-^{3}H]glucose, together with the disintegrations per minute of phosphorylated [^{3}H]deoxyglucose from individual muscles, were used to calculate insulin-stimulated glucose metabolic index (Rg′), an estimate of tissue glucose uptake (28).

Biochemical assays

During clamps, plasma was immediately obtained from withdrawn blood by centrifugation and frozen for subsequent insulin determination (rat insulin RIA; Linco Research Inc., St. Charles, MO) and total adiponectin determination by ELISA (rat adiponectin ELISA; Millipore) according to the manufacturer's instructions. Triglyceride was extracted from TCMs (29) and quantified using triglyceride reagent and calibrator (Microgenics, Fremont, CA). Muscle glycogen and lactate were extracted and analyzed as previously described (30, 31). Rate of synthesis of glycogen was determined from the D-[U-^{14}C]glucose disappearance curve and counts of [^{14}C] in the extracted muscle glycogen as previously described (28).

Real-time PCR

mRNA transcript levels were quantified using real-time PCR assay. TCMs were powdered under liquid nitrogen and homogenized using an Ultra-Turrax (IKA, Staufen, Germany) in Trizol (Invitrogen, Paisley, UK). Total RNA was then extracted as per the manufacturer's instructions and resuspended in nuclease-free water. RNA concentration and purity were assessed using a Nanodrop 1000 (Wilmington, DE) and integrity confirmed by visualization of rRNA bands after agarose gel electrophoresis. Genomic DNA contamination of RNA preparations was eliminated by digestion with ribonuclease-free deoxyribonuclease, and then cDNA was generated using an Omniscript kit (QIAGEN). Real-time PCR analysis was per-

formed using Fast Start SYBR Green reagent (Roche Diagnostics, Burgess Hill, UK) on a Chromo4 detector (Bio-Rad Laboratories, Hemel Hempstead, UK), with normalization to fluorescence from the passive reference dye ROX. Reaction mixtures contained 20 ng of cDNA, 1.5 μM each primer, and 2.5–5 mM $MgCl_2$, as required, and were subjected to a 10-min hot start, followed by 40–45 cycles of 15 sec at 95 C, 30 sec at 55–61 C, and 30 sec at 72 C and a final 5-min extension. Primer pairs (supplied by Invitrogen or Sigma-Aldritch) were designed using the Primer 3 program (http://frodo.wi.mit.edu) and are listed, together with the optimized PCR conditions for each, in Supplemental Table 1, published on The Endocrine Society's Journals Online web site at http://endo.endojournals.org. The relative abundance of duplicate cDNA aliquots was quantified using a standard curve plotted from amplification of a 10-fold dilution series of DNA generated by conventional PCR from the same primer pairs and gel purified as previously described (32). Results are quoted after normalization to the mRNA level of cyclophilin, the expression of which was unchanged by the treatments. Generation of a single appropriate PCR product was confirmed by melting curve analysis after each amplification and periodic agarose gel electrophoresis.

Muscle lysates, subcellular fractionation, SDS-PAGE, and immunoblotting

Protein expression and phosphorylation of molecules present in muscle was assessed by SDS-PAGE and quantification of Western blots of a minimum of n = 6 tissue lysates, typically in duplicate. Whole-muscle lysates were prepared from powdered muscle by homogenization using the Ultra-Turrax (IKA) in radioimmunoprecipitation assay (RIPA) buffer [65 mmol/liter Tris, 150 mmol/liter NaCl, 5 mmol/liter EDTA (pH 7.4), 1% (vol/vol) Igepal-CA630 detergent, 0.5% (wt/vol) sodium deoxycholate, 0.1% (wt/vol) sodium dodecyl sulfate, 10% (vol/vol) glycerol, containing 25 μg/ml leupeptin, 10 μg/ml aprotinin, 2 mmol/liter sodium orthovanadate, 10 mmol/liter NaF, 2.5 mM sodium pyrophosphate, and 1 mmol/liter polymethylsulfonyl fluoride] followed by rotation for 90 min at 4 C, centrifugation for 10 min at 16,000 $\times$ *g*, and collection of the supernatant. Subcellular fractionation was carried out using a method adapted from Lizunov *et al.* (33), incorporating an additional homogenization and centrifugation of the 800-g pellet, with the combination of the two supernatants, and the use of the protease/phosphatase inhibitors listed above. The high-speed pellet (HSP) generated, representing a crude membrane preparation, was used for immunoblotting.

Protein content of lysate supernatants or subcellular fractions was quantified using the bicinchoninic acid method (Pierce Biotechnology Inc., Rockford, IL) using a BSA standard, normalized to the lowest concentration and denatured in Laemmli buffer for 10 min at 65 C. Aliquots containing 20–80 μg protein were resolved by SDS-PAGE, electrotransferred, and immunoblotted as previously described (34). Specific bands were detected using chemoluminescence (Western Lightning Plus; PerkinElmer, Seer Green, UK) on Fuji Super RX film (Bedford, UK), scanned, and quantified by local background-adjusted volume measurement using Quantity One software (Bio-Rad Laboratories). Data for phosphorylated and total content for each protein target are shown separately, with anti-β actin blots for each set of muscle lysates used as a loading control.

Assay of sphingolipid analysis by liquid chromatography-mass spectrometry (LC-MS)

Sphingolipidomics was performed as described previously (35). Powdered TCMs obtained from chow and HFD-fed rats were homogenized in PBS using the Ultra-Turrax (IKA), and lysates were cleared by centrifugation at 13,000 $\times$ *g*. To 40 μl of each lysate was added 0.75 ml of methanol-chloroform (2:1) and an internal standard cocktail containing 500 pmol each of C12-Sphingomyelin, C17-Ceramide, C8-Dihydroceramide, C17-Sphingosine, and C12-Glucosylceramide (Avanti Polar Lipids, Alabaster, AL). This single-phase mixture was probe sonicated for 30 sec at room temperature and then incubated overnight at 48 C. After cooling to room temperature, 75 μl of 1 M KOH in methanol was added, followed by incubation at 37 C for 2 h. Lipids were neutralized with 4 μl glacial acetic acid and partitioned into an organic phase by adding 1 ml of chloroform and 2 ml of distilled H_2O, followed by thorough mixing and centrifugation at 1000 $\times$ *g* for 5 min. The upper phase was reextracted with 1 ml of chloroform and the two lower (organic) phases pooled to obtain the final extract. This was dried under nitrogen and reconstituted in mobile phase solvent [acetonitrile/methanol/formic acid 97/2/1 (vol/vol/vol), containing 5 mM ammonium formate] for liquid chromatography-tandem mass spectrometry. Samples were subjected to normal phase LC-MS using a 4000Qtrap mass spectrometer (Applied Biosystems, Carlsbad, CA) and a multiple reaction monitoring scheme for naturally occurring species of ceramide, sphingomyelin, hexosylceramide, and sphingosine. Data acquisition was performed as described (35) and normalized to protein content (determined using the bicinchoninic acid method).

Statistics

Data are quoted as mean $\pm$ SE. Comparisons between treated and control muscles in the same animal were made

using paired Student's *t* tests and between chow and HFD rats using unpaired *t* tests. Comparisons between HFD and chow fed rats subsequently electroporated were made by two-way ANOVA with one repeated measure (comparison between limbs). *Post hoc* analysis was undertaken using the Holm-Sidak test, together, where appropriate, with the paired or unpaired Student's *t* test to elucidate interactions. Analyses were conducted using Sigma Stat version 3.00 (SPSS Inc., Chicago, IL), with $P < 0.05$ regarded as significant.

Results

Overexpression of AdipoR1 in TCMs of rats

IVE was used to introduce a plasmid expressing AdipoR1 cDNA into right and an empty plasmid into left TCMs of rats. One week later, Western blotting of muscle lysates demonstrated an approximate 4.5-fold increase in AdipoR1 protein in test *vs.* paired control muscles (Fig. 1A), confirming successful OE of the receptor. In addition, subcellular fractionation and subsequent blotting of the HSP (crude membrane fraction) confirmed that this overexpression was present in cellular membranes (Fig. 1A). A separate cohort of rats was either chow or HFD fed for 6 wk, with IVE being performed 1 wk before a HEC and euthanasia. In these animals, an approximate 3-fold OE of AdipoR1 was generated, irrespective of the diet fed, with no HFD-induced impairment of AdipoR1 protein expression being noted in control muscles (Fig. 1B). Total plasma adiponectin levels measured in fasted animals before clamping were similar between chow and HFD-fed rats and within the expected range (Table 1).

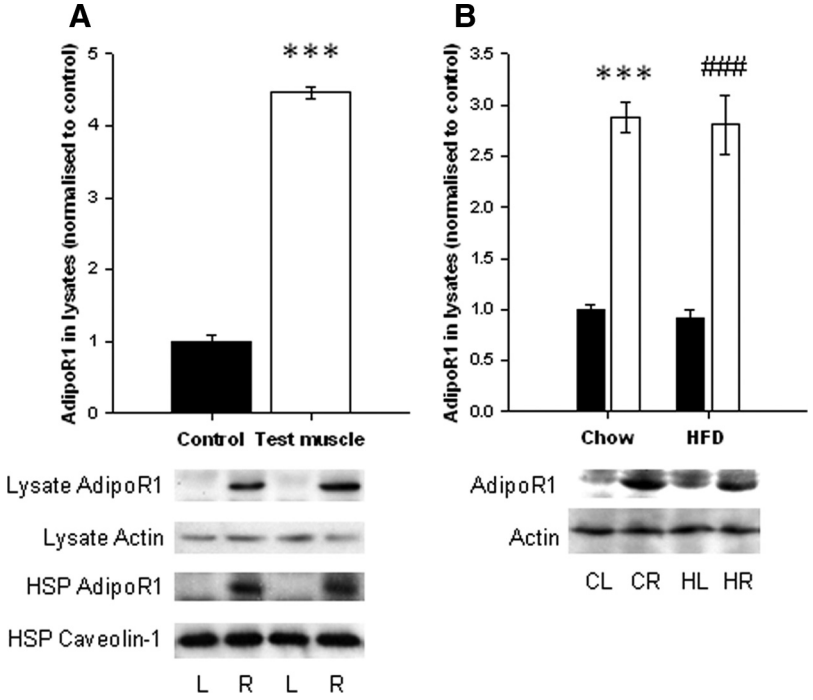

FIG. 1. Overexpression of AdipoR1 in single TCMs of rats by *in vivo* electrotransfer (IVE). IVE of an AdipoR1 cDNA-containing construct was used to over-express AdipoR1 expression in TCMs of chow-fed rats (**A**) and separate cohorts of rats that were either fed on a HFD or chow for 6 wk (B). One week later, successful overexpression of AdipoR1 was demonstrated by immunoblotting of tissue lysates and HSP (membrane fractions) derived from the test and control TCMs. Typical immunoblots for AdipoR1 in test (*right panel*, R, *white bars*) and paired control (*left panel*, L, *black bars*) muscles from HFD- (HL and HR) and chow (CL and CR)-fed rats are shown along with blots of β-actin and the membrane-specific protein caveolin-1 to demonstrate equal loading in lysates and HSP, respectively. Paired *t* testing: ***, $P < 0.001$ *vs.* chow-fed control; ###, $P < 0.001$ *vs.* HFD-fed control muscles. Data are mean ± SEM (n = 8–20).

AdipoR1 OE causes increased muscle glucose disposal through activation of the insulin signaling pathway

To assess glucose disposal into paired AdipoR1 overexpressing and control muscles 1 wk after IVE, 2-deoxyglucose tracer uptake, lactate, and glycogen content were measured. Glucose uptake was increased by 46% ($P = 0.015$; Fig. 2A), lactate content was reduced by 22% ($P = 0.003$; Fig. 2B), and glycogen storage was increased by 17% ($P = 0.0011$; Fig. 2C) as a result of AdipoR1 OE. Consistent with these findings, phosphorylation of phosphatidylinositol 3-kinase (PI3-kinase) signaling intermediates IRS1 (pY608), Akt (pS473), and GSK3β (pS9) were all increased (Fig. 2, D and E), suggesting that AdipoR1 OE causes glycogen accumulation by disinhibition of glycogen synthesis. In addition, AdipoR1 OE also caused small increases in total protein levels of IRS1 and GSK3β in the absence of any change in β-actin expression.

AdipoR1 OE increases insulin-stimulated glucose disposal into muscle in both chow- and HFD-fed rats

To investigate whether the effect of AdipoR1 OE on glucose disposal into muscle would be additive to that of insulin, HEC combined with bolus administration of 2-[1,2-^{3}H (N)]-deoxy-D-glucose and D-[U-^{14}C]glucose was conducted. Half of the rats were fed a HFD for 6 wk before HEC to establish whether muscle AdipoR1 OE would be sufficient to overcome local lipid-associated IR. As predicted, HFD feeding resulted in increases in basal plasma

TABLE 1. Chow- and HFD-fed rat characteristics mean (SEM) under basal and hyperinsulinemic-euglycemic clamp conditions

	Chow fed		HFD fed	
	Basal	Clamp	Basal	Clamp
Plasma glucose (mM)	7.0 (0.2)	7.2 (0.3)	8.0 (0.2)[a]	7.1 (0.4)
Plasma insulin (pM)	184 (18)	1992 (197)	461 (64)[b]	1928 (98)
Body mass at study (g)	362 (9)		422 (7)[b]	
Epididymal fat pad mass (% body mass)	0.55 (0.06)		0.95 (0.13)[c]	
Plasma adiponectin (μg/ml)	13.4 (0.3)		12.1 (0.4)	
Glucose infusion rate (mg/kg·min)		43.8 (3.2)		22.4 (2.7)[b]
Whole-body R_d (mg/kg·min)		36.2 (1.8)		21.8 (1.6)[b]
Endogenous glucose output (mg/kg·min)		−7.5 (2.4)		−0.6 (1.4)[c]

[a] $P < 0.01$ *vs.* equivalent measurement for chow-fed rats (n = 6–15).
[b] $P < 0.001$ *vs.* equivalent measurement for chow-fed rats (n = 6–15).
[c] $P < 0.05$ *vs.* equivalent measurement for chow-fed rats (n = 6–15).

glucose and insulin, total body mass, and fat mass, as indicated by a 73% increase in the epididymal fat pad as a percentage of body mass (Table 1). This diet also reduced clamp GIR and R_d and increased endogenous glucose output, despite equivalent clamp plasma glucose and insulin concentrations (insulin ~1.9–2.0 nM; Table 1 and Fig. 3, A and B). Insulin-stimulated glucose uptake and glucose incorporation into glycogen during the last 45 min of the clamp, as well as glycogen content at the end of the clamp, were all reduced in TCMs as a result of HFD feeding (Fig. 3, C–E). However, increases in each parameter were generated by prior AdipoR1 OE, irrespective of feeding status. This effect was relatively modest for glucose uptake but more marked for glycogen synthesis and storage. Thus, although a HFD did not negatively impact AdipoR1 levels, OE of this receptor was capable of enhancing insulin-stimulated glucose disposal in both normal and insulin resistant muscle and thus also of partially ameliorating IR in this tissue.

Increased glucose disposal is associated with an additive effect of AdipoR1 OE to that of insulin on phosphorylation of insulin signaling pathway intermediates

To establish whether AdipoR1 OE activated the PI3-kinase pathway, phosphorylation and protein expression levels of signaling intermediates were measured in muscle lysates from clamped rats. HFD significantly impaired both Ser473-Akt and total Akt protein levels, without affecting pY608-IRS1, pS9-GSK3β, or pT642-TBC1D4 (Fig. 4). This apparent lack of an effect of HFD feeding on insulin signaling is typical after about 2.5 h insulin infusion (18). Despite these muscles having been subjected to high physiological levels of insulin for this period, phosphorylation of all the signaling intermediates measured was still increased by AdipoR1 OE (Fig. 4), consistent with the effects of AdipoR1 OE under basal insulin conditions (Fig. 2). AdipoR1 OE also resulted in increased total levels of all these signaling proteins.

Muscle AdipoR1 OE results in increased AMPK phosphorylation and increased levels of target proteins

To establish the effects of AdipoR1 OE on the AMPK signaling pathway and downstream targets pertinent to muscle mitochondrial function, further Western blotting was undertaken. First, phosphorylation of p70S6 kinase was assessed at the Thr389 residue, the target site for the mammalian target of rapamycin, because reduced activation of this kinase has been implicated in the activation of AMPK by adiponectin in myoblasts (36). However, AdipoR1 OE in fact caused an increase in phosphorylation at this site, consistent with its effect to increase flux through the type I PI3-kinase pathway, but there was also a trend ($P = 0.058$) for this to be increased by HFD feeding (Fig. 5A), as previously observed (37). As predicted and in line with PI3-kinase signaling data, phosphorylation of AMPK (Thr172) was increased by AdipoR1 OE (Fig. 5B), and a broadly consistent effect was also observed in phosphorylation of acetyl-coA carboxylase (ACC) at the AMPK target residue (Ser79), particularly due to an increase in the HFD-fed animals (Fig. 5C; interaction $P = 0.074$). Total ACC protein was also increased in AdipoR1 OE muscles. Downstream of AMPK, protein levels of PGC1α (Fig. 5D) and UCP3 (Fig. 5E) were also increased by AdipoR1 OE, irrespective of dietary status, whereas UCP3 levels were further increased by HFD feeding. These changes are likely indicative of increased mitochondrial oxidative activity but potentially decreased efficiency, consistent with previously published mouse data (38). In addition, protein levels of APPL1 (Fig. 5F) and adiponectin (Fig. 5G) were increased in AdipoR1 OE muscles.

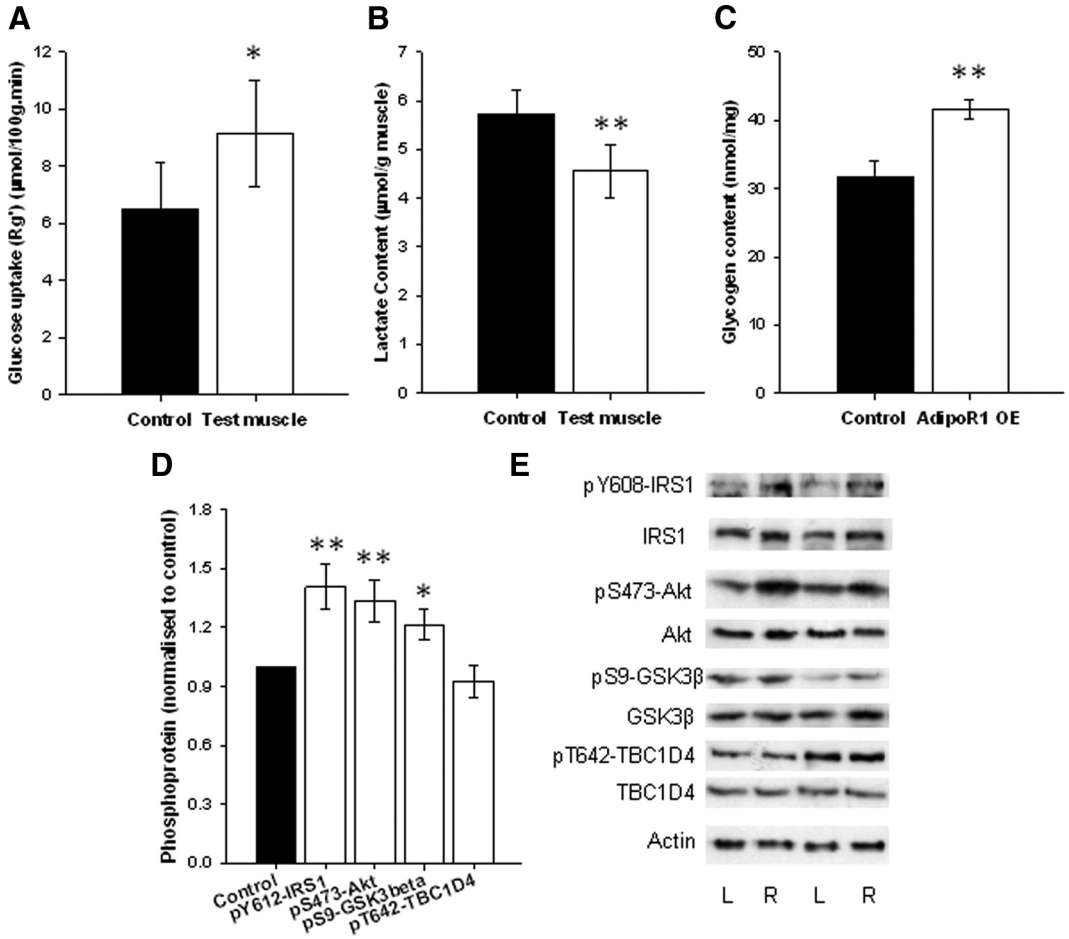

FIG. 2. AdipoR1 overexpression causes increased glucose disposal into muscle, associated with increased phosphorylation of PI3-kinase pathway intermediates, under basal insulin conditions. One week after IVE, basal 2-deoxyglucose uptake tracer uptake was measured in paired AdipoR1-overexpressing and paired control TCMs of 5-h-starved rats. Using snap-frozen muscle from euthanized animals, lysates were generated and used in Western immunoblotting for phosphorylated and total PI3-kinase signaling intermediates, and glycogen and lactate content were measured. A, Glucose uptake was increased as a result of AdipoR1 OE. B, Lactate content was decreased. C, However, glycogen content was increased by AdipoR1 OE. D, Summary of effects of AdipoR1 OE on phosphorylation of IRS1 (pY608), Akt (pS473), GSK3β (pS9), and TBC1D4 (pT642), normalized to the contralateral control muscle. All except pT642-TBC1D4 were increased by the manipulation. E, Typical immunoblots of phosphorylated and total IRS1, Akt, GSK3β, and TBC1D4, with actin as the loading control. There were small increases in protein levels of both total IRS1 and GSK3β, in the absence of any change in actin levels. L, Left; R, right. Paired *t* testing: *, $P < 0.05$, **, $P < 0.01$ *vs.* control. Data are mean ± SEM (n = 6–12).

AdipoR1 OE reduces muscle content of specific sphingolipid species

To assess altered sphingolipid content as a potential mechanistic factor in the insulin-sensitizing effects of AdipoR1 OE in muscle, we undertook a comprehensive sphingolipidomic screen by LC-MS of muscles from chow- and HFD-fed rats after clamping. A complete set of mean data for each sphingolipid species detected is shown as Supplemental Table 2, whereas the most notable changes induced by AdipoR1 OE are shown in Fig. 6. Although most sphingolipid species were maintained in their normal range despite HFD feeding or AdipoR1 OE, the levels of certain individual species were regulated by AdipoR1 OE. Levels of both total ceramide and saturated ceramide were unaltered, but unsaturated ceramide tended to be reduced by AdipoR1 OE in the muscle of chow-fed rats (interaction $P = 0.084$; Fig. 6A). In further contrast to the data collected from adiponectin-treated mouse liver described by Holland *et al.* (14), S1P levels were increased by the HFD but significantly reduced in both chow and HFD-fed rats after AdipoR1 OE (Fig. 6B), with similar effects on total sphingosine (see Supplemental Table 2). AdipoR1 OE caused a reduction in ceramide 18:1 (Fig. 6C), ceramide 20:2 (Fig. 6D) and dihydroceramide 20:0 (Fig. 6E), consistent with a putative, but selective, ceramidase activity of the receptor (14). Of these sphingolipids, only ceramide 18:1 was affected by diet ($P = 0.055$). In contrast, ceramide 22:0 showed a small reduction in AdipoR1 OE muscles from chow-fed rats but the opposite change in HFD-fed rats (Fig. 6F), whereas sphingomyelin 20:1 was increased by AdipoR1 OE in chow-fed rats and reduced by this manipulation in HFD-fed rats (Fig. 6G).

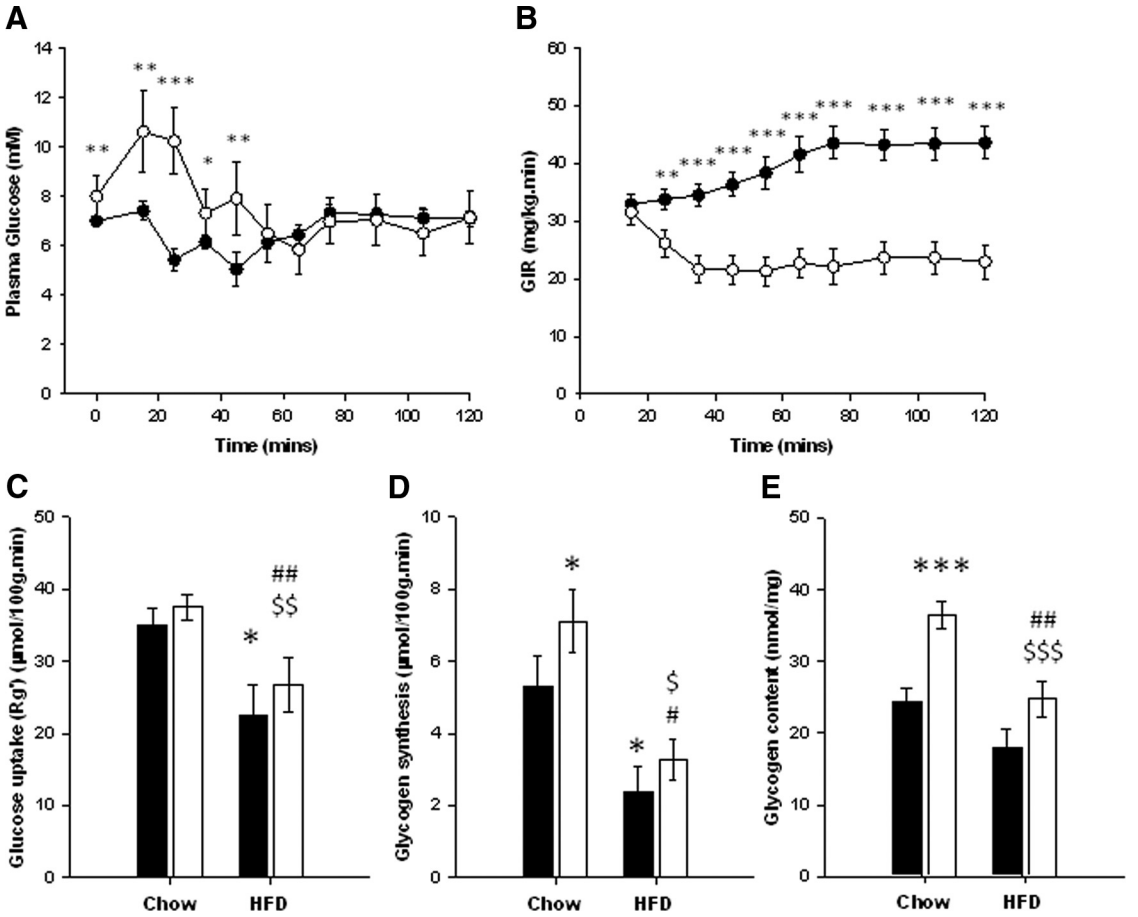

FIG. 3. AdipoR1 overexpression enhances glucose disposal and glycogen storage in normal and HFD-fed rats. AdipoR1 was overexpressed in the right TCMs of groups of rats that had been fed for 6 wk on a HFD or chow. One week later, rats were subjected to hyperinsulinemic-euglycemic clamp combined with the administration of radiolabeled glucose and 2-deoxyglucose tracer. Expected patterns of plasma glucose concentration (A) and GIR (B) throughout the clamp are shown for chow- and HFD-fed rats. TCMs were collected after euthanasia at the end of the procedure and, together with whole-body glucose flux and plasma tracer disappearance curves, were used to measure glucose uptake (C), glucose incorporation into glycogen during the clamp (D) and glycogen content in AdipoR1-overexpressing and paired control muscles (E). *White bars*, AdipoR1 overexpressing muscles; *black bars*, contralateral control muscles. By two-way repeated-measures ANOVA, there were overall reductions in all of these parameters as a result of HFD feeding ($P = 0.008$, $P = 0.012$, and $P = 0.006$, respectively) and increases, irrespective of feeding status, in muscles that were overexpressing AdipoR1 ($P = 0.039$, $P = 0.009$, and $P < 0.001$, respectively). The *post hoc* changes are displayed as follows: *, $P < 0.05$, **, $P < 0.01$, ***, $P < 0.001$ *vs.* chow-fed rats or their muscles; #, $P < 0.05$, ##, $P < 0.01$ *vs.* HFD-fed control muscles; $, $P < 0.05$, $$, $P < 0.01$, $$$, $P < 0.001$ *vs.* chow-fed test muscles. Data are mean ± SEM (n = 7–13).

Altered sphingolipid content of muscle is associated with changes in expression of key sphingolipid metabolizing enzymes

Synthesis and metabolism of sphingolipid species is mediated by a series of membrane-associated enzymes, whose activity is at least partially regulated at the transcriptional level (39). To investigate whether the observed selective changes in muscle sphingolipid species abundance were dictated by changes in enzyme expression, we measured mRNA levels of a range of these by quantitative PCR. Despite the lack of increase in ceramide levels observed in the rat muscles, both HFD feeding and AdipoR1 OE had similar effects to increase expression of ceramide synthase (CS)-1 but not CS4 (Fig. 7A). However, further downstream in the ceramide synthetic pathway, expression of both glucosylceramide synthase (Fig. 7B), serine palmitoyl transferase (SPTS) subunit 2 (Fig. 7C, but not subunit 1) and sphingolipid Δ4 desaturase (Fig. 7D) were decreased by AdipoR1 OE in both chow- and HFD-fed rat muscle, consistent with the AdipoR1-mediated reductions in some but not the majority of the sphingolipid species detected. Consistent with the reduction in S1P levels, S1P lyase mRNA was increased in the chow-fed animals, although this change was abolished in the HFD-fed animals (Fig. 7E). However, an observed increase in S1P phosphatase mRNA, perhaps denoting secondary activation of the ceramide salvage pathway (39) may be responsible for the reduced S1P levels in the HFD-fed rats (see Fig. 7F).

Discussion

In this manuscript, we have demonstrated that local overexpression of AdipoR1 causes an increase in disposal of

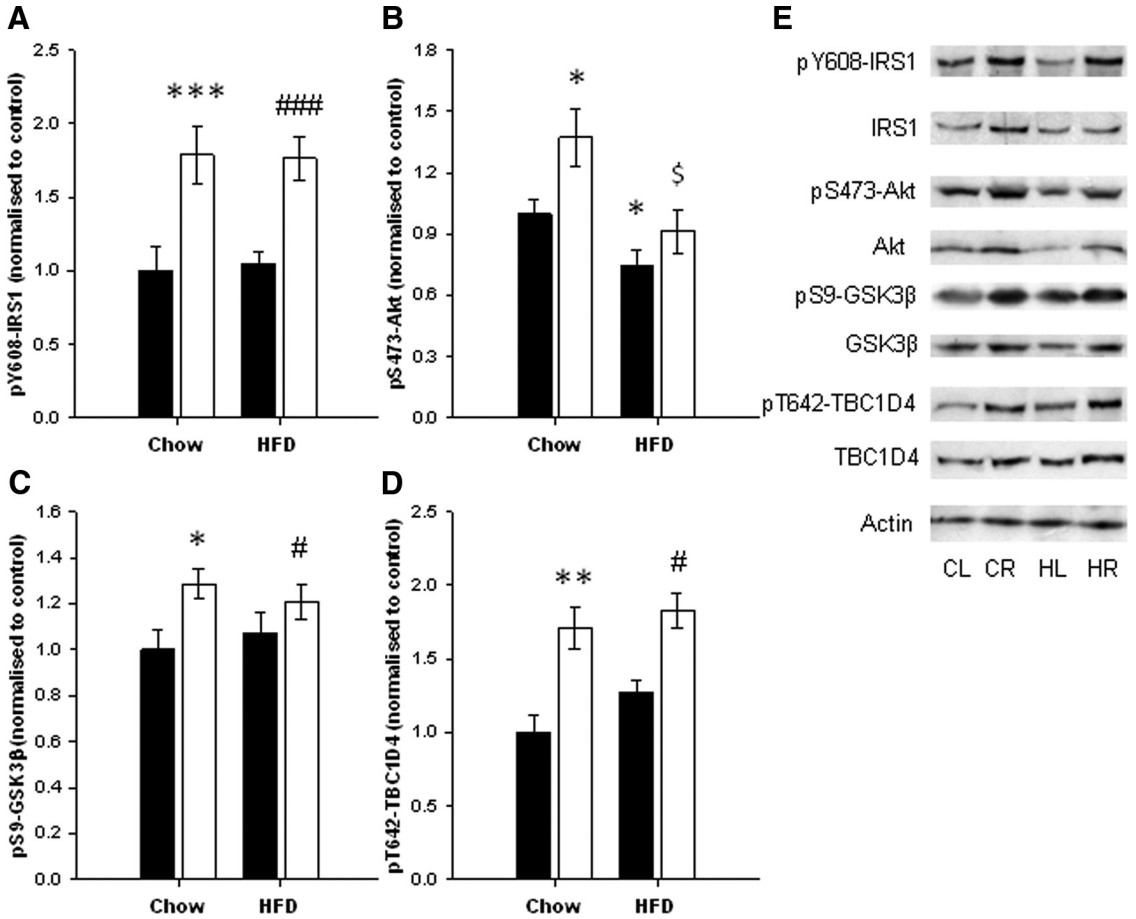

FIG. 4. The increased muscle insulin sensitivity is mediated through increased phosphorylation and protein levels of PI3-kinase pathway signaling intermediates. Lysates were prepared from paired TCMs collected from rats at the termination of a HEC and subjected to SDS-PAGE and western immunoblotting for phosphorylation and total levels of PI3-kinase signaling intermediates. A, pY608-IRS1 was increased as a result of AdipoR1 overexpression in chow- and HFD-fed rats (ANOVA, $P < 0.001$). B, pS473-Akt was also increased by AdipoR1 OE (ANOVA, $P = 0.015$) but decreased by HFD (ANOVA, $P = 0.004$). Both pS9-GSK3β (C) and pT642-TBC1D4 (D) were also increased by AdipoR1 OE (ANOVA, $P = 0.004$ and $P < 0.001$, respectively). E, Typical immunoblots for phosphorylated and total proteins in test [right (R), *white bars*] and paired control [left (L), *black bars*] muscles from HFD- (HL and HR) and chow (CL and CR)-fed rats. IRS1, Akt, GSK3β, and TBC1D4 protein were all increased by AdipoR1 OE, whereas Akt was also decreased by HFD feeding according to ANOVA. Levels of the housekeeping protein actin were unchanged by either treatment. *Post hoc* changes are displayed as follows: *, $P < 0.05$, **, $P < 0.01$, ***, $P < 0.001$ *vs.* chow-fed control; #, $P < 0.05$, ###, $P < 0.001$ *vs.* HFD-fed control muscles; $, $P < 0.05$ *vs.* chow-fed test muscles. Data are mean ± SEM (n = 8 per group).

glucose into skeletal muscle, associated with both increased flux through the insulin signaling pathway and activation of AMPK. This effect occurred under basal conditions but also, additively, under the insulin-stimulated conditions of a HEC. Furthermore, this effect was observed in both normal and insulin-resistant muscle, implying that AdipoR1 OE is capable of both insulin-mimetic activity and of partially ameliorating HFD-induced defects in muscle glucose disposal *in vivo*. We have obtained these findings by acute manipulation of gene expression in single adult rat muscles, using *in vivo* electrotransfer (26). This technique largely avoids the potential for developmental or whole-body compensation, which are inherent to germline methods of genetic manipulation, but by the same token, the conclusions drawn relate to muscle-autonomous effects. This clearly has a bearing on the interpretation of the data with respect to other studies conducted using traditional transgenic technologies.

Much clinical data exist that demonstrate an inverse correlation between plasma adiponectin concentrations and IR/obesity (6, 7, 10), and a number of studies have demonstrated an insulin-sensitizing effect of administered adiponectin at the whole-body (40, 41) and muscle cell/tissue level (8, 9, 42). However, it is unclear to what extent tissue sensitivity to adiponectin rather than ligand concentration determines this effect *in vivo*. In this study, we have used OE of AdipoR1, the principal adiponectin receptor in skeletal muscle, to increase local adiponectin sensitivity in muscle of rats. Importantly, test and control muscles from individual rats were exposed to identical plasma adiponectin concentrations. HFD feeding did not af-

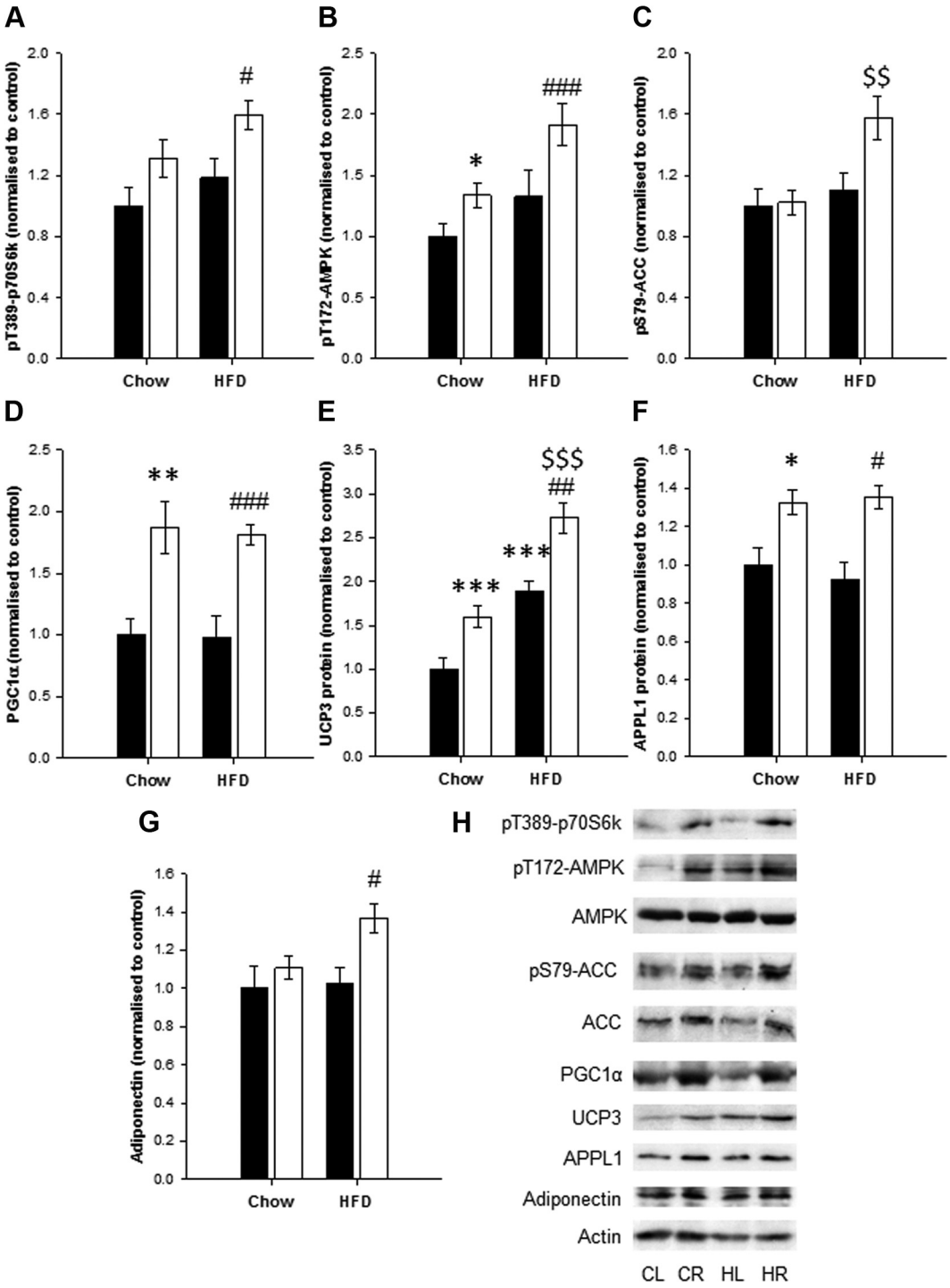

FIG. 5. AdipoR1 overexpression increases p70S6 kinase and AMPK phosphorylation and levels of mitochondrial proteins. Lysates were prepared from paired TCMs collected from rats at the termination of a hyperinsulinemic-euglycemic clamp and subjected to SDS-PAGE and Western immunoblotting for levels of phosphorylated and total proteins. A, pT389–p70S6 kinase was increased as a result of AdipoR1 OE (ANOVA, $P = 0.011$) and tended to increase as a result of HFD feeding also ($P = 0.058$). B, pT172-AMPK was also increased by AdipoR1 OE (ANOVA, $P < 0.001$). C, pS79-ACC was increased by HFD feeding ($P = 0.009$) and by AdipoR1 OE ($P = 0.050$), principally due to an effect in HFD-fed rats (interaction, $P = 0.074$). PGC1α protein was also increased by AdipoR1 OE (D) (ANOVA, $P < 0.001$), as was UCP3 protein (E) (ANOVA, $P < 0.001$), although this was also increased by HFD feeding ($P < 0.001$). APPL1 protein was also increased by AdipoR1 OE (F) (ANOVA, $P < 0.001$), as was adiponectin (G) (ANOVA, $P = 0.008$). H, Typical immunoblots for phosphorylated and total proteins in test [right (R), *white bars*] and paired control [left (L), *black bars*] muscles from HFD- (HL and HR) and chow (CL and CR)-fed rats. Total ACC protein was also increased by AdipoR1 OE but unaffected by HFD feeding according to ANOVA. The levels of the housekeeping protein actin were unchanged by either treatment. The *post hoc* changes are displayed as follows: *, $P < 0.05$, **, $P < 0.01$, ***, $P < 0.001$ *vs.* chow-fed control; #, $P < 0.05$, ##, $P < 0.01$, ###, $P < 0.001$ *vs.* HFD-fed control muscles; $$, $P < 0.01$, $$$, $P < 0.001$ *vs.* chow-fed test muscles. Data are mean ± SEM (n = 8 per group).

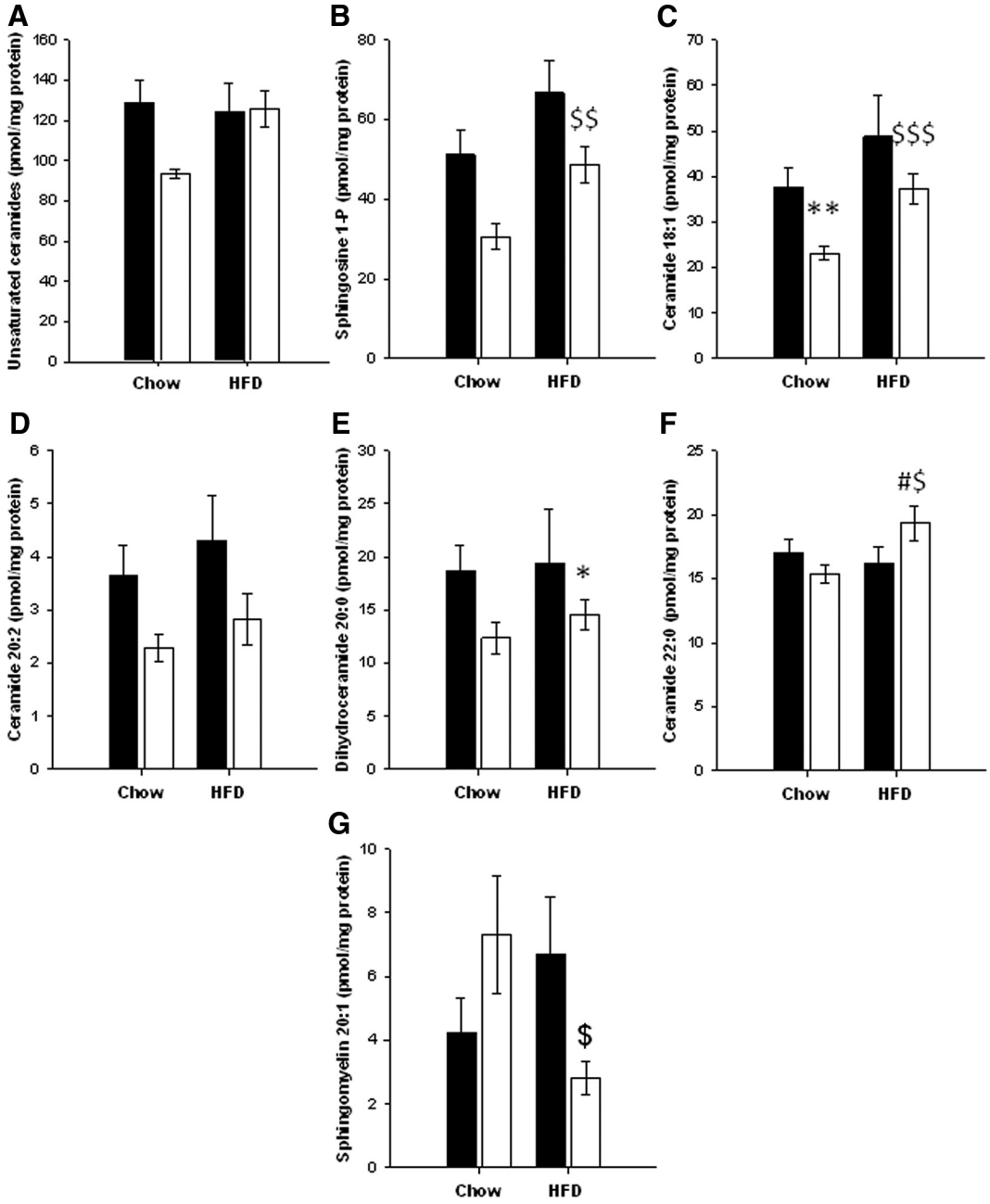

FIG. 6. Improved insulin signaling is associated with a reduction in specific sphingolipid species in AdipoR1-overexpressing muscles. Content of selected sphingolipid species (picomoles per milligram of protein) of AdipoR1-overexpressing (OE) and paired control TCMs removed from chow and HFD-fed rats after hyperinsulinemic-euglycemic clamp. Species showing changes as a result of AdipoR1 OE are shown here. A comprehensive list of sphingolipids detected in right and left muscles from each group of rats is shown as Supplemental Table 2. A, Whereas there was no difference in the content of total saturated ceramide between groups, there was a trend toward a reduction in total unsaturated ceramide in the chow-fed rats (interaction, $P = 0.084$). B, Sphingosine-1 phosphate was increased by HFD feeding (ANOVA, $P = 0.005$) but reduced by AdipoR1 OE ($P = 0.016$). With regard to individual sphingolipid species of note, ceramide 18:1 (C) showed a similar trend due to diet ($P = 0.055$) and was reduced by AdipoR1 OE ($P = 0.020$). Ceramide 20:2 (D) ($P = 0.031$) and dihydroceramide 20:0 (E) ($P = 0.036$) were also reduced by AdipoR1 OE. In contrast, ceramide 22:0 (F) was reduced by AdipoR1 OE in chow-fed rats but increased by this manipulation in HFD-fed rats (interaction, $P = 0.018$), whereas sphingomyelin 20:1 (G) was increased by AdipoR1 OE in chow-fed rats and decreased by this manipulation in HFD-fed rats (interaction, $P = 0.034$). Mean (SEM) is shown (n = 6–10). The *post-hoc* differences are displayed as follows: *, $P < 0.05$, **, $P < 0.01$ *vs.* control chow-fed rats; #, $P < 0.05$ *vs.* HFD-fed control muscles; $, $P < 0.05$, $$, $P < 0.01$, $$$, $P < 0.001$ *vs.* chow-fed test muscles.

fect total plasma adiponectin measured before a HEC, consistent with a previous report using a very similar model (43).

Phosphorylation of AMPK, a key downstream mediator of adiponectin action in muscle (20), was increased by AdipoR1 OE in both chow- and HFD-fed rats, confirming the success of our approach. In fact, adiponectin sensitization had positive effects on glucose disposal under basal, insulin-stimulated, and insulin-resistant conditions. In-

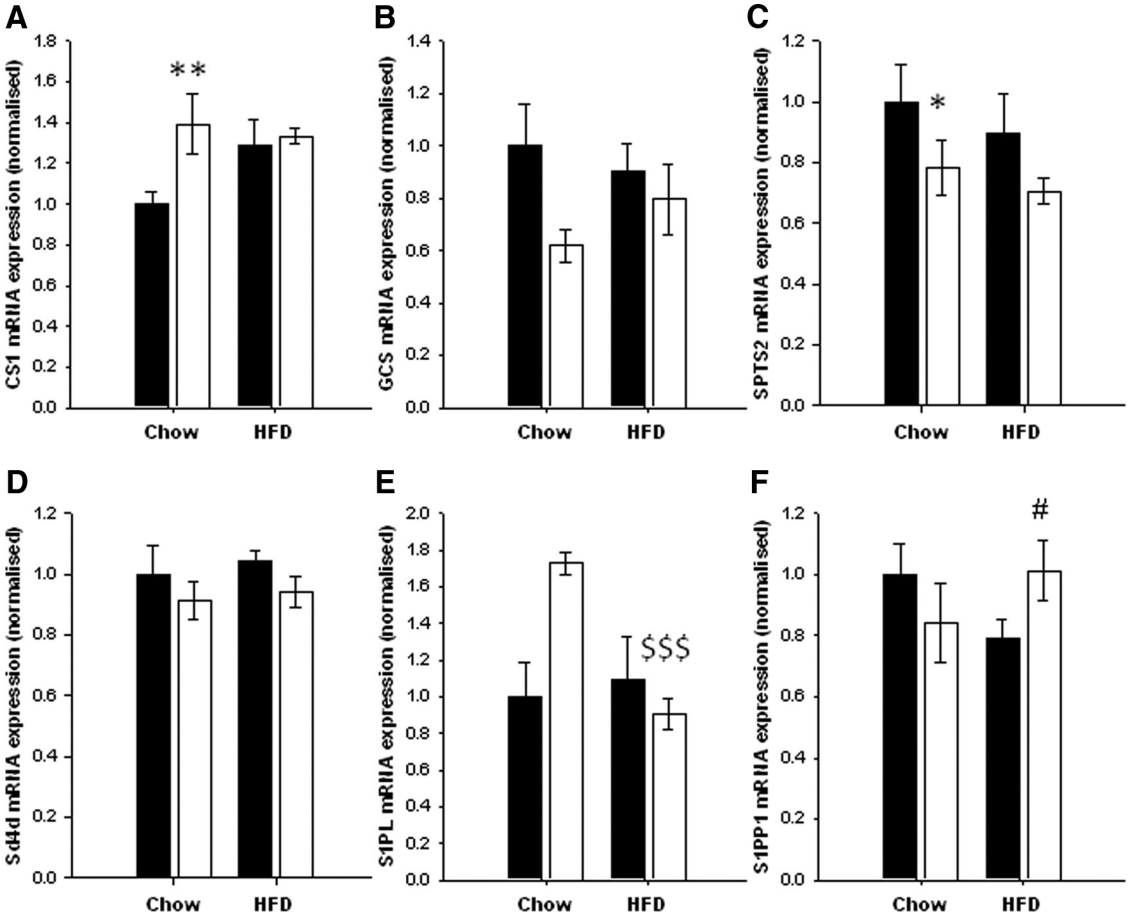

FIG. 7. The altered sphingolipid profile is associated with consistent changes in expression of sphingolipid metabolizing enzymes. mRNA expression of sphingolipid metabolizing enzymes in AdipoR1-overexpressing (OE) and paired control TCMs removed from chow- and HFD-fed rats after hyperinsulinemic-euglycemic clamp were quantified using real-time RT-PCR. Neither treatment affected mRNA levels of the reference genes 36B4 or cyclophilin. A, CS1 was increased by AdipoR1 OE (ANOVA, $P = 0.003$) but also similarly by HFD feeding (interaction, $P = 0.007$). Glucosyl ceramide synthase (GCS) (B), SPTS2 (C), and sphingolipid-δ4 desaturase (Sd4d) (D) were reduced overall by AdipoR1 OE (ANOVA, $P = 0.030$, $P = 0.022$, and $P = 0.027$, respectively). Sphingosine 1-phosphate lyase (S1PL) was increased by AdipoR1 OE in chow-fed muscles only (E) (ANOVA interaction, $P = 0.032$), whereas sphingosine 1-phosphate phosphatase-1 (S1PP1) mRNA was reduced by HFD feeding (F), but this change was normalized by AdipoR1 OE (ANOVA interaction, $P = 0.036$). No changes in expression of SPTS1, acid ceramidase, ceramide kinase-1, or ceramide synthase-4 were noted (data not shown). Mean (SEM) is shown (n = 7–10). The *post-hoc* differences are displayed as follows: *, $P < 0.05$, **, $P < 0.01$ *vs.* control chow-fed rats; #, $P < 0.05$ *vs.* HFD-fed control muscles; $$$, $P < 0.001$ *vs.* chow-fed test muscles.

creased glucose uptake was associated with increased glycogen accumulation in AdipoR1 muscle, with glycogen storage being favored over complete glycolysis to lactate. These results partially contrast with previous data showing an effect of globular adiponectin to increase glucose uptake and lactate synthesis at the expense of glycogen synthesis as well as increased fatty oxidation, but not glucose oxidation as a result of this treatment, in L6 myotubes (44). These disparities may relate to the use of a cell line and of globular adiponectin in the previous study. We did not measure glucose oxidation in this study, but altered AdipoR1 levels may also have impacted on this pathway. Although some previous reports have shown increased AdipoR1 mRNA as a result of HFD feeding (45, 46), we saw no effect of a HFD at the protein level. Despite this, however, AdipoR1 OE had an insulin-sensitizing effect because it partially ameliorated the HFD-induced impairment in acute muscle glucose uptake and the glycogen synthesis and normalized glycogen storage in the rats in this study, associated with increases in phosphorylation and expression of multiple intermediates in the PI3-kinase signaling pathway.

The intracellular pathway linking ligand binding by AdipoR1 to its metabolic effects of increased glucose disposal and mitochondrial activity is not fully characterized, although AMPK activation, as demonstrated here, seems to be an important downstream component. There was a modest increase in adiponectin in AdipoR1 OE muscles, which may simply reflect increased binding in the presence of increased receptor. Binding of AdipoR1 to the adaptor protein APPL1 has been suggested to play a role in the antiapoptotic effect of adiponectin in endothelial cells (47)

and the ERK-mediated stimulation of cell growth (48) by the use of AdipoR1 silencing *in vitro* but has also been implicated in the insulin sensitizing effect of adiponectin by generating a node for cross talk between adiponectin and insulin signaling pathways (19). This contention is supported by the strikingly similar effects that we have observed on glucose disposal and both phosphorylation and protein expression levels of the PI3-kinase pathway intermediates as a result of OE of AdipoR1 in this study and of APPL1 previously (18). Here we show that APPL1 expression is increased in clamped AdipoR1-overexpressing muscles; hence, some of the effects of AdipoR1 may be mediated through increased APPL1 and/or an increased level of the interaction between AdipoR1 and APPL1.

The level at which APPL1 interacts with the PI3-kinase pathway in this model is as yet unclear. APPL1 has been shown to interact directly with Akt (49), but IRS1 phosphorylation is also increased by either APPL1 or AdipoR1 OE upstream of this putative interaction (this manuscript and Ref. 18). Although it has been proposed that adiponectin may insulin sensitize through reduced serine phosphorylation of IRS1 by p70S6 kinase (36), our *in vivo* data are not consistent with this model. AMPK activation has been proposed to be mediated through intercompartmental translocation of its activating kinase, liver kinase B1, in response to APPL1 binding (50) and also via triggering of an intracellular calcium influx, resulting in activation of a second AMPK kinase, CAMKKβ (17). AdipoR1 was shown to be required in muscle for this latter mechanism, and AdipoR1 deficiency resulted in decreased PGC1α and consequently reduced mitochondrial activity. Consistent with this, adiponectin overexpression was recently shown to amplify mitochondrial biogenesis in muscle via increased PGC1α expression (51), findings that are complementary to our own.

An alternative mechanism for adiponectin action was proposed by Holland *et al.* in 2011 (14), based on data showing that the AdipoRs possess an inherent ceramidase activity, which when activated metabolizes tissue ceramide to sphingosine. A reduction in muscle ceramide would be expected to have beneficial effects on insulin sensitivity by removing its inhibitory effects on insulin signaling (3). In our study, IR was induced by HFD feeding in the absence of any elevation in whole-muscle ceramide levels. Whereas these data contradict the findings of a number of studies (reviewed in Ref. 3), the role of ceramide accumulation in the etiology of muscle IR is not fully established. Indeed, studies in humans have variously suggested ceramide levels were or were not associated with muscle IR (for a review, see Ref. 52), whereas elevated total muscle IR can develop in rodents in the absence of changes in ceramide concentration (53). However, the type of fat ingested seems to be important because a diet rich in saturated FA tends to result in increased ceramide levels in red muscle, but increased dietary unsaturated FA does not (54). The diet used in this study and many others is lard based, containing principally C16:0, C18:0, C18:1, and C18:2 fatty acids, but with two thirds of the FA content by mass being unsaturated. In addition, it is possible that a longer duration of HFD feeding may have resulted in increased muscle ceramide levels, and potentially this might have permitted an observable effect of AdipoR1 OE, whereas different results may also have been observed in mouse or human muscle or in a muscle in which type I (oxidative) fibers predominate (*e.g.* in the soleus), rather than in the predominantly glycolytic TCM, because obesity is associated with a preferential deposition of ceramide in this fiber type (55). By the same token, differential overexpression of AdipoR1 between fiber types, due to variations in either transfection efficiency or promoter activity, could have played a role. Finally, it is unclear how subcellular localization of sphingolipids or idiosyncratic sphingolipid species contributes to the pathology of IR (3).

Whereas 6 wk HFD feeding did not cause a general elevation in sphingolipids, including ceramide, there was an effect to increase muscle S1P levels. Reductions in levels of SPTS2 mRNA, sphingolipid δ-4 desaturase mRNA, several ceramide species (particularly 18:1 and 20:2) and S1P suggest that altered sphingolipid metabolism may be implicated in the mechanism for the positive effects of AdipoR1 OE on glucose disposal and insulin sensitivity in muscle. In addition to a HFD-mediated increase in S1P, we also showed an AdipoR1-related reduction in this signaling molecule, which may be explained by increased activation of the ceramide salvage pathway, indicated by elevated S1PP1 and ceramide synthase expression, because S1PL expression was in fact reduced by AdipoR1. This change may not be quantitatively important because expression levels of S1PL are reportedly low in muscle (56). However, because ceramide levels were largely unchanged or reduced by AdipoR1 OE, the fate of the ceramide produced in this way is uncertain. In a previous study, palmitate treatment of C2C12 myoblasts caused increased ceramide via *de novo* synthesis and increased S1P via activation of sphingosine kinase-1 (57). In the same study, HFD feeding with an identical diet also caused an increase in sphingosine kinase-1 mRNA.

A sphingolipid rheostat, comprising inversely regulated S1P and ceramide concentrations, has been proposed to regulate the cellular balance between growth/differentiation and apoptosis via a series of intracellular S1P receptors (58). Here the S1P to ceramide ratio was increased by HFD feeding but decreased by AdipoR1 OE, which according to this hypothesis would tend to favor apoptosis

over growth/differentiation and thus be unlikely to mediate improved insulin sensitivity. These data also run contrary to the effect of S1P accumulation to increase glucose disposal previously observed in myoblasts and diabetic mice (59). S1P also enhances the mobilization of calcium from the endoplasmic reticulum, which might therefore result in AMPK activation via its upstream kinase CAMKKβ (17). However, AMPK activation was enhanced by AdipoR1 OE, suggesting that this mechanism is also not likely to be responsible. In addition, our data are not consistent with the model that adiponectin-induced AMPK activation is mediated by the upstream generation of S1P generation in muscle, as previously hypothesized (14). Instead, a possible explanation is that AdipoR1 OE might ameliorate HFD-induced insulin resistance through a reduction in the S1P-mediated local inflammation, as previously suggested (56).

We are confident that the reductions in Sphingosine and S1P we detected in AdipoR1-overexpressing muscles are genuine because all sphingolipid species were analyzed in the same liquid chromatography-tandem mass spectrometry assay, in which most classes of sphingolipids remained unchanged. Currently it is unclear what role sphingosine and S1P may play in insulin sensitivity. The relative disconnect between the changes in gene expression observed and the small changes in the sphingolipid profile suggests that more significant regulation of sphingolipid levels may be occurring downstream of the mRNA level. The increase in CS1 may be a compensatory response to regenerate C18 and C20 sphingolipids, which tend to be decreased in AdipoR1 OE muscles. Furthermore, because the effects on PI3-kinase signaling intermediates occurred from the level of IRS1 down, whereas ceramide inhibition of insulin signaling is thought to be mediated by protein phosphatase 2A-mediated dephosphorylation of (60) and PKC-dependent inhibition of binding of phosphoinositide to Akt (61), altered sphingolipid metabolism is unlikely to be the sole mechanism for the beneficial effects of AdipoR1 OE.

In conclusion, we have demonstrated a direct role for adiponectin action via AdipoR1 in the enhancement of insulin sensitivity in skeletal muscle *in vivo*. This effect involves activation of the PI3-kinase and AMPK signaling pathways and is associated with selective changes in muscle sphingolipid content. Thus, therapeutic measures aimed at enhancing adiponectin signaling in skeletal muscle may have a beneficial effect in the treatment of conditions such as T2D, which are underpinned by IR.

Acknowledgments

We are indebted to Quintin Lau, Emma Polkinghorne, and Tracie Reinten (Garvan Institute) and Rachel Robertson (Royal Veterinary College) for technical assistance; the staff of the Biological Services Unit (Royal Veterinary College) for animal care; and Associate Professor Asish Saha (Boston University) for advice on the lactate assay. Anti-AdipoR1 antibody, the anti-APPL1 antibody, and the pCAGGS vector were kind gifts from Astra Zeneca (Mölndal, Sweden), Professor Aimin Xu (University of Hong Kong), and Professor Dominic Wells (Royal Veterinary College, University of London), respectively.

Address all correspondence and requests for reprints to: Dr. Mark E. Cleasby, Department of Comparative Biomedical Sciences, Royal Veterinary College, University of London, Royal College Street, London NW1 0TU, United Kingdom. E-mail: mcleasby@rvc.ac.uk.

This work was supported by the Wellcome Trust (Grant 087461), the National Health and Medical Research Council of Australia (Grant 481303), and Diabetes UK (Small Grant 07/0003540). M.E.C. is a Wellcome Trust University Award Fellow. N.T. is supported by a Career Development Award and E.W.K., J.P.W., and G.J.C. by Research Fellowships from the National Health and Medical Research Council. K.L.H. is supported by an American Diabetes Association Junior Faculty Award.

Disclosure Summary: The authors have nothing to disclose.

References

1. **Hegarty BD, Furler SM, Ye J, Cooney GJ, Kraegen EW** 2003 The role of intramuscular lipid in insulin resistance. Acta Physiol Scand 178:373–383
2. **Erion DM, Shulman GI** 2010 Diacylglycerol-mediated insulin resistance. Nat Med 16:400–402
3. **Summers SA** 2010 Sphingolipids and insulin resistance: the five Ws. Curr Opin Lipidol 21:128–135
4. **Dyck DJ** 2009 Adipokines as regulators of muscle metabolism and insulin sensitivity. Appl Physiol Nutr Metab 34:396–402
5. **Sell H, Dietze-Schroeder D, Eckel J** 2006 The adipocyte-myocyte axis in insulin resistance. Trends Endocrinol Metab 17:416–422
6. **Lara-Castro C, Luo N, Wallace P, Klein RL, Garvey WT** 2006 Adiponectin multimeric complexes and the metabolic syndrome trait cluster. Diabetes 55:249–259
7. **Pajvani UB, Hawkins M, Combs TP, Rajala MW, Doebber T, Berger JP, Wagner JA, Wu M, Knopps A, Xiang AH, Utzschneider KM, Kahn SE, Olefsky JM, Buchanan TA, Scherer PE** 2004 Complex distribution, not absolute amount of adiponectin, correlates with thiazolidinedione-mediated improvement in insulin sensitivity. J Biol Chem 279:12152–12162
8. **Fang X, Palanivel R, Zhou X, Liu Y, Xu A, Wang Y, Sweeney G** 2005 Hyperglycemia- and hyperinsulinemia-induced alteration of adiponectin receptor expression and adiponectin effects in L6 myoblasts. J Mol Endocrinol 35:465–476
9. **Mullen KL, Smith AC, Junkin KA, Dyck DJ** 2007 Globular adiponectin resistance develops independently of impaired insulin-stimulated glucose transport in soleus muscle from high-fat-fed rats. Am J Physiol Endocrinol Metab 293:E83–E90
10. **Weyer C, Funahashi T, Tanaka S, Hotta K, Matsuzawa Y, Pratley RE, Tataranni PA** 2001 Hypoadiponectinemia in obesity and type 2 diabetes: close association with insulin resistance and hyperinsulinemia. J Clin Endocrinol Metab 86:1930–1935
11. **Segal KR, Landt M, Klein S** 1996 Relationship between insulin sen-

sitivity and plasma leptin concentration in lean and obese men. Diabetes 45:988–991
12. **Lin HV, Kim JY, Pocai A, Rossetti L, Shapiro L, Scherer PE, Accili D** 2007 Adiponectin resistance exacerbates insulin resistance in insulin receptor transgenic knockout mice. Diabetes 56:1969–1976
13. **Yamauchi T, Kamon J, Ito Y, Tsuchida A, Yokomizo T, Kita S, Sugiyama T, Miyagishi M, Hara K, Tsunoda M, Murakami K, Ohteki T, Uchida S, Takekawa S, Waki H, Tsuno NH, Shibata Y, Terauchi Y, Froguel P, Tobe K, Koyasu S, Taira K, Kitamura T, Shimizu T, Nagai R, Kadowaki T** 2003 Cloning of adiponectin receptors that mediate antidiabetic metabolic effects. Nature 423: 762–769
14. **Holland WL, Miller RA, Wang ZV, Sun K, Barth BM, Bui HH, Davis KE, Bikman BT, Halberg N, Rutkowski JM, Wade MR, Tenorio VM, Kuo MS, Brozinick JT, Zhang BB, Birnbaum MJ, Summers SA, Scherer PE** 2011 Receptor-mediated activation of ceramidase activity initiates the pleiotropic actions of adiponectin. Nat Med 17:55–63
15. **Bjursell M, Ahnmark A, Bohlooly-Y M, William-Olsson L, Rhedin M, Peng XR, Ploj K, Gerdin AK, Arnerup G, Elmgren A, Berg AL, Oscarsson J, Lindén D** 2007 Opposing effects of adiponectin receptors 1 and 2 on energy metabolism. Diabetes 56:583–593
16. **Yamauchi T, Nio Y, Maki T, Kobayashi M, Takazawa T, Iwabu M, Okada-Iwabu M, Kawamoto S, Kubota N, Kubota T, Ito Y, Kamon J, Tsuchida A, Kumagai K, Kozono H, Hada Y, Ogata H, Tokuyama K, Tsunoda M, Ide T, Murakami K, Awazawa M, Takamoto I, Froguel P, Hara K, Tobe K, Nagai R, Ueki K, Kadowaki T** 2007 Targeted disruption of AdipoR1 and AdipoR2 causes abrogation of adiponectin binding and metabolic actions. Nat Med 13:332–339
17. **Iwabu M, Yamauchi T, Okada-Iwabu M, Sato K, Nakagawa T, Funata M, Yamaguchi M, Namiki S, Nakayama R, Tabata M, Ogata H, Kubota N, Takamoto I, Hayashi YK, Yamauchi N, Waki H, Fukayama M, Nishino I, Tokuyama K, Ueki K, Oike Y, Ishii S, Hirose K, Shimizu T, Touhara K, Kadowaki T** 2010 Adiponectin and AdipoR1 regulate PGC-1α and mitochondria by Ca(2+) and AMPK/SIRT1. Nature 464:1313–1319
18. **Cleasby ME, Lau Q, Polkinghorne E, Patel SA, Leslie SJ, Turner N, Cooney GJ, Xu A, Kraegen EW** 2011 The adaptor protein APPL1 increases glycogen accumulation in rat skeletal muscle through activation of the PI3-kinase signalling pathway. J Endocrinol 210: 81–92
19. **Mao X, Kikani CK, Riojas RA, Langlais P, Wang L, Ramos FJ, Fang Q, Christ-Roberts CY, Hong JY, Kim RY, Liu F, Dong LQ** 2006 APPL1 binds to adiponectin receptors and mediates adiponectin signalling and function. Nat Cell Biol 8:516–523
20. **Yamauchi T, Kamon J, Minokoshi Y, Ito Y, Waki H, Uchida S, Yamashita S, Noda M, Kita S, Ueki K, Eto K, Akanuma Y, Froguel P, Foufelle F, Ferre P, Carling D, Kimura S, Nagai R, Kahn BB, Kadowaki T** 2002 Adiponectin stimulates glucose utilization and fatty-acid oxidation by activating AMP-activated protein kinase. Nat Med 8:1288–1295
21. **Zhou L, Deepa SS, Etzler JC, Ryu J, Mao X, Fang Q, Liu DD, Torres JM, Jia W, Lechleiter JD, Liu F, Dong LQ** 2009 Adiponectin activates AMPK in muscle cells via APPL1/LKB1- and PLC/Ca2+/CaMKK-dependent pathways. J Biol Chem 284:22426–22435
22. **Bruce CR, Mertz VA, Heigenhauser GJ, Dyck DJ** 2005 The stimulatory effect of globular adiponectin on insulin-stimulated glucose uptake and fatty acid oxidation is impaired in skeletal muscle from obese subjects. Diabetes 54:3154–3160
23. **Niwa H, Yamamura K, Miyazaki J** 1991 Efficient selection for high-expression transfectants with a novel eukaryotic vector. Gene 108: 193–199
24. **Cheng KK, Lam KS, Wang Y, Huang Y, Carling D, Wu D, Wong C, Xu A** 2007 Adiponectin-induced endothelial nitric oxide synthase activation and nitric oxide production are mediated by APPL1 in endothelial cells. Diabetes 56:1387–1394
25. **Bruce CR, Hoy AJ, Turner N, Watt MJ, Allen TL, Carpenter K, Cooney GJ, Febbraio MA, Kraegen EW** 2009 Overexpression of carnitine palmitoyltransferase-1 in skeletal muscle is sufficient to enhance fatty acid oxidation and improve high fat diet-induced insulin resistance. Diabetes 58:550–558
26. **Cleasby ME, Davey JR, Reinten TA, Graham MW, James DE, Kraegen EW, Cooney GJ** 2005 Acute bidirectional manipulation of muscle glucose uptake by *in vivo* electrotransfer of constructs targeting glucose transporter genes. Diabetes 54:2702–2711
27. **Kraegen EW, James DE, Bennett SP, Chisholm DJ** 1983 *In vivo* insulin sensitivity in the rat determined by euglycemic clamp. Am J Physiol 245:E1–E7
28. **Kraegen EW, James DE, Jenkins AB, Chisholm DJ** 1985 Dose-response curves for *in vivo* insulin sensitivity in individual tissues in rats. Am J Physiol 248:E353–E362
29. **Bligh EG, Dyer WJ** 1959 A rapid method of total lipid extraction and purification. Can J Med Sci 37:911–917
30. **Chan TM, Exton JH** 1976 A rapid method for the determination of glycogen content and radioactivity in small quantities of tissue or isolated hepatocytes. Anal Biochem 71:96–105
31. **Gutmann I, Wahlefeld AW, Bergmeyer HU** 1974 L-(+)-lactate determination with lactate dehydrogenase and NAD. In: Methods of enzymatic analysis. Vol 3. New York: Weinheim and Academic Press; 1464–1468
32. **Polkinghorne E, Lau Q, Cooney GJ, Kraegen EW, Cleasby ME** 2008 Local activation of the IκK-NFκB pathway in muscle does not cause insulin resistance. Am J Physiol Endocrinol Metab 294:E316–E325
33. **Lizunov VA, Stenkula KG, Lisinski I, Gavrilova O, Yver DR, Chadt A, Al-Hasani H, Zimmerberg J, Cushman SW** 2012 Insulin stimulates fusion, but not tethering, of GLUT4 vesicles in skeletal muscle of HA-GLUT4-GFP transgenic mice. Am J Physiol Endocrinol Metab 302:E950–E960
34. **Cleasby ME, Dzamko N, Hegarty BD, Cooney GJ, Kraegen EW, Ye JM** 2004 Metformin prevents the development of acute lipid-induced insulin resistance in the rat through altered hepatic signaling mechanisms. Diabetes 53:3258–3266
35. **Shaner RL, Allegood JC, Park H, Wang E, Kelly S, Haynes CA, Sullards MC, Merrill Jr AH** 2009 Quantitative analysis of sphingolipids for lipidomics using triple quadrupole and quadrupole linear ion trap mass spectrometers. J Lipid Res 50:1692–1707
36. **Wang C, Mao X, Wang L, Liu M, Wetzel MD, Guan KL, Dong LQ, Liu F** 2007 Adiponectin sensitizes insulin signaling by reducing p70 S6 kinase-mediated serine phosphorylation of IRS-1. J Biol Chem 282:7991–7996
37. **Um SH, Frigerio F, Watanabe M, Picard F, Joaquin M, Sticker M, Fumagalli S, Allegrini PR, Kozma SC, Auwerx J, Thomas G** 2004 Absence of S6K1 protects against age- and diet-induced obesity while enhancing insulin sensitivity. Nature 431:200–205
38. **Turner N, Bruce CR, Beale SM, Hoehn KL, So T, Rolph MS, Cooney GJ** 2007 Excess lipid availability increases mitochondrial fatty acid oxidative capacity in muscle: evidence against a role for reduced fatty acid oxidation in lipid-induced insulin resistance in rodents. Diabetes 56:2085–2092
39. **Bruni P, Donati C** 2008 Pleiotropic effects of sphingolipids in skeletal muscle. Cell Mol Life Sci 65:3725–3736
40. **Yamauchi T, Kamon J, Waki H, Terauchi Y, Kubota N, Hara K, Mori Y, Ide T, Murakami K, Tsuboyama-Kasaoka N, Ezaki O, Akanuma Y, Gavrilova O, Vinson C, Reitman ML, Kagechika H, Shudo K, Yoda M, Nakano Y, Tobe K, Nagai R, Kimura S, Tomita M, Froguel P, Kadowaki T** 2001 The fat-derived hormone adiponectin reverses insulin resistance associated with both lipoatrophy and obesity. Nat Med 7:941–946
41. **Satoh H, Nguyen MT, Trujillo M, Imamura T, Usui I, Scherer PE, Olefsky JM** 2005 Adenovirus-mediated adiponectin expression augments skeletal muscle insulin sensitivity in male Wistar rats. Diabetes 54:1304–1313
42. **Yoon MJ, Lee GY, Chung JJ, Ahn YH, Hong SH, Kim JB** 2006 Adiponectin increases fatty acid oxidation in skeletal muscle cells by

sequential activation of AMP-activated protein kinase, p38 mitogen-activated protein kinase, and peroxisome proliferator-activated receptor α. Diabetes 55:2562–2570

43. **Amengual-Cladera E, Lladó I, Gianotti M, Proenza AM** 2012 Sex differences in the effect of high-fat diet feeding on rat white adipose tissue mitochondrial function and insulin sensitivity. Metabolism 61:1108–1117
44. **Ceddia RB, Somwar R, Maida A, Fang X, Bikopoulos G, Sweeney G** 2005 Globular adiponectin increases GLUT4 translocation and glucose uptake but reduces glycogen synthesis in rat skeletal muscle cells. Diabetologia 48:132–139
45. **Barnea M, Shamay A, Stark AH, Madar Z** 2006 A high-fat diet has a tissue-specific effect on adiponectin and related enzyme expression. Obesity (Silver Spring) 14:2145–2153
46. **Bullen Jr JW, Bluher S, Kelesidis T, Mantzoros CS** 2007 Regulation of adiponectin and its receptors in response to development of diet-induced obesity in mice. Am J Physiol Endocrinol Metab 292: E1079–E1086
47. **Park M, Youn B, Zheng XL, Wu D, Xu A, Sweeney G** 2011 Globular adiponectin, acting via AdipoR1/APPL1, protects H9c2 cells from hypoxia/reoxygenation-induced apoptosis. PLoS One 6:e19143
48. **Lee MH, Klein RL, El-Shewy HM, Luttrell DK, Luttrell LM** 2008 The adiponectin receptors AdipoR1 and AdipoR2 activate ERK1/2 through a Src/Ras-dependent pathway and stimulate cell growth. Biochemistry 47:11682–11692
49. **Saito T, Jones CC, Huang S, Czech MP, Pilch PF** 2007 The interaction of AKT with APPL1 is required for insulin-stimulated Glut4 translocation. J Biol Chem 282:32280–32287
50. **Deepa SS, Zhou L, Ryu J, Wang C, Mao X, Li C, Zhang N, Musi N, DeFronzo RA, Liu F, Dong LQ** 2011 APPL1 mediates adiponectin-induced LKB1 cytosolic localization through the PP2A-PKCζ signaling pathway. Mol Endocrinol 25:1773–1785
51. **Qiao L, Kinney B, Yoo HS, Lee B, Schaack J, Shao J** 2012 Adiponectin increases skeletal muscle mitochondrial biogenesis by suppressing mitogen-activated protein kinase phosphatase-1. Diabetes 61:1463–1470
52. **Coen PM, Dubé JJ, Amati F, Stefanovic-Racic M, Ferrell RE, Toledo FG, Goodpaster BH** 2010 Insulin resistance is associated with higher intramyocellular triglycerides in type I but not type II myocytes concomitant with higher ceramide content. Diabetes 59:80–88
53. **Hoy AJ, Brandon AE, Turner N, Watt MJ, Bruce CR, Cooney GJ, Kraegen EW** 2009 Lipid and insulin infusion-induced skeletal muscle insulin resistance is likely due to metabolic feedback and not changes in IRS-1, Akt, or AS160 phosphorylation. Am J Physiol Endocrinol Metab 297:E67–E75
54. **Blachnio-Zabielska A, Baranowski M, Zabielski P, Gorski J** 2010 Effect of high fat diet enriched with unsaturated and diet rich in saturated fatty acids on sphingolipid metabolism in rat skeletal muscle. J Cell Physiol 225:786–791
55. **Kristensen D, Prats C, Larsen S, Ara I, Dela F, Helge JW** 21 February 2012 Ceramide content is higher in type I compared to type II fibers in obesity and type 2 diabetes mellitus. Acta Diabetol 10.1007/500592-012-0379-0
56. **Serra M, Saba JD** 2010 Sphingosine 1-phosphate lyase, a key regulator of sphingosine 1-phosphate signaling and function. Adv Enzyme Regul 50:349–362
57. **Hu W, Bielawski J, Samad F, Merrill Jr AH, Cowart LA** 2009 Palmitate increases sphingosine-1-phosphate in C2C12 myotubes via upregulation of sphingosine kinase message and activity. J Lipid Res 50:1852–1862
58. **Spiegel S, Milstien S** 2003 Sphingosine-1-phosphate: an enigmatic signalling lipid. Nat Rev Mol Cell Biol 4:397–407
59. **Ma MM, Chen JL, Wang GG, Wang H, Lu Y, Li JF, Yi J, Yuan YJ, Zhang QW, Mi J, Wang L, Duan HF, Wu CT** 2007 Sphingosine kinase 1 participates in insulin signalling and regulates glucose metabolism and homeostasis in KK/Ay diabetic mice. Diabetologia 50: 891–900
60. **Schmitz-Peiffer C, Craig DL, Biden TJ** 1999 Ceramide generation is sufficient to account for the inhibition of the insulin-stimulated PKB pathway in C2C12 skeletal muscle cells pretreated with palmitate. J Biol Chem 274:24202–24210
61. **Powell DJ, Hajduch E, Kular G, Hundal HS** 2003 Ceramide disables 3-phosphoinositide binding to the pleckstrin homology domain of protein kinase B (PKB)/Akt by a PKCζ-dependent mechanism. Mol Cell Biol 23:7794–7808